Available online at www.sciencedirect.com
ScienceDirect
Vacuum 82 (2008) 651–656
VACUUM
SURFACE ENGINEERING, SURFACE INSTRUMENTATION & VACUUM TECHNOLOGY
www.elsevier.com/locate/vacuum

A spectroscopic study into the decomposition process of titanium isopropoxide in the nitrogen–hydrogen 100 kHz low-pressure plasma

P. Jamroz, W. Zyrnicki*

Chemistry Department, Wroclaw University of Technology, Wyb. Wyspianskiego 27, 50-370 Wroclaw, Poland

Received 11 June 2007; received in revised form 25 September 2007; accepted 9 October 2007

Abstract

Optical emission spectroscopy was employed for the study of the nitrogen–hydrogen and nitrogen–hydrogen–titanium (IV) isopropoxide mixtures in the 100 kHz low pressure capacitively coupled discharge. High-energy species were identified in the plasma phase. The behavior of the excited species versus the gas composition has also been investigated. The optical actinometry technique was applied in order to evaluate the N_2, CH, CO, CN, N, C and the H relative concentrations versus the hydrogen concentration in reactive mixtures. The effect of the hydrogen concentration in the nitrogen–hydrogen mixture on the decomposition processes of titanium isopropoxide was investigated. The plasma temperature (the H excitation temperature, the CN, N_2 and N_2^+ vibrational temperatures and the N_2^+ rotational temperature) as well as the electron number density were determined here. The temperature magnitudes ($T_{exc} \approx 5700$–7400 K, $T_{vib}(CN) \approx 4700$–8100 K, $T_{vib}(N_2) \approx 2700$–$3050$ K, $T_{vib}(N_2^+) \approx 1500$–$1600$ K and $T_{rot}(N_2^+) \approx 660$–$890$ K) indicated a very significant deviation from the LTE state.

Keywords: Plasma diagnostics; Optical emission spectroscopy; Plasma-assisted chemical vapor deposition; Titanium isopropoxide

1. Introduction

The plasma-assisted chemical vapor deposition (PACVD) methods, using the easy volatile metal organic compounds (MO)-PACVD, are widely applied for the production of many kinds of coatings and thin layers [1]. Among them, titanium nitride (TiN) and thin layers of titanium carbon nitride (TiCN, TiCNO) are very interesting as regards their mechanical, electrical, anticorrosive and decorative properties [2–4].

Normally, titanium chloride ($TiCl_4$) is applied for the production of TiN or TiCNO coatings (e.g. [4–8]). However, chlorine impurities may affect the properties of the thin layers [3]. Alternatively, easy volatile MO, such as titanium tetraisopropoxide (TIP) [3,9–11], tetrakis dimethylamidotitanium (TDMAT) [12,13], tetrakis diethylamidotitanium (TDEAT) [3], diethylaminotitanium (DEAT) [14], dimethylaminotitanium (DMAT) [15], have been used recently to deposit titanium nitride or thin layers of titanium carbon nitride. Weber et al. [2,9] have shown that thin films of high quality TiN are produced from titanium (IV) isopropoxide–nitrogen microwave plasma at a low substrate temperature. Multi-component TiCNO layers were also produced [10,11] from the direct current (dc) TIP–N_2–H_2 plasma on the Armco-iron steel.

In order to understand the plasma chemistry of the PACVD processes, it is necessary to know the conditions occurring in the plasma phase and the concentrations of species in the excited states as well as in the ground states. The plasma parameters (i.e. the temperature, the concentrations of high energy species, the electron number density) are very important from the point of view of the processes leading to the formation of thin layers. The plasma diagnostics may appear very useful for the understanding of the deposition process. Optical emission spectroscopy (OES) as well as optical actinometry, due to their non-invasive character, have been used as tools for plasma diagnostics and for investigating the PACVD processes [1,5,6,16–19]. The OES technique was frequently

*Corresponding author. Tel./fax: +48 71 3202494.
E-mail address: wieslaw.zyrnicki@pwr.wroc.pl (W. Zyrnicki).

0042-207X/$ - see front matter © 2007 Elsevier Ltd. All rights reserved.
doi:10.1016/j.vacuum.2007.10.003

applied in order to study and control the plasma TiN, TiCN and TiCNO deposition processes [3–6,8,10,18]. However, only a few papers are concerned with the investigation of the MO-PACVD processes by means of OES in system containing titan MO. Boo et al. [3] analyzed the radical formation and ionization behaviors in plasma containing tetrakis diethylamidotitanium by means of OES. Wierzchon and Sobiecki [10] investigated the emission spectra of selected species, i.e. CN, Ti, Ti^+, versus the cathode temperature in the dc titanium isopropoxide plasma. In their earlier work, Kulakowska-Pawlak and Zyrnicki [18] studied the dc glow discharge in the reactive mixture containing titanium isopropoxide. They found that emission intensities of active species were sensitive to changes in the plasma gas composition and the cathode temperature.

The main aim of this work is to obtain information on the decomposition process of TIP in the mid-frequency nitrogen–hydrogen plasma, while the former studies [10,18] concerned the dc discharges. The glow discharges in the nitrogen–hydrogen–TIP and in the nitrogen–hydrogen mixtures were characterized by OES as well as by the optical actinometry technique. The plasma parameters, i.e. plasma temperatures (excitation, vibrational and rotational) and electron number density at various mixture compositions were also investigated.

2. Experimental setup

Mid-frequency power supply (100 kHz, 100 mA, 200 W) was employed here to generate low-pressure plasma in the reactive mixture. The plasma was excited in a Pyrex glass cylindrical reactor chamber between two parallel Armco-iron electrodes (diameter: 22 mm, thickness: 2 mm, distance between the electrodes: 16 mm). The chamber had water cooled walls and a quartz window enabling observation of the plasma radiation spectrum. A schematic diagram of the experimental setup was described in the earlier work [17].

Titanium (IV) tetraisopropoxide (chemical formula $Ti[OCH(CH_3)_2]_4$, purity 97%, purchased from Aldrich-Sigma) was introduced by means of a bubbler system to the plasma reactor with a stream of gases. The evaporation temperature of TIP (60 °C) was controlled with the aid of the thermostat. The gas line connecting the bubbler system with the plasma reactor was additionally heated to about 60 °C in order to avoid the condensation of a titanium MO on the cold walls of the pipeline. The flow rate of TIP was constant and kept at the level of $0.04\,g\,min^{-1}$ ($140\,\mu mol\,min^{-1}$).

A mixture of nitrogen and hydrogen was used as a carrier gas. The percentage of hydrogen in the mixture was as follows: 0, 25, 50, 75 and 100. The flow rate of reactive gases was regulated with the aid of flow meters (Tylan General). The pressure was kept constant (532 Pa) and controlled by means of a pressure gauge (Pfeiffer). The gas mixture was pumped continuously by a rotational pump device. A cryogenic trap (liquid nitrogen) in the front of vacuum pump system was additionally applied.

The radiation emitted by the plasma was measured by a JY TRIAX 320 ($f = 32$ cm, resolution 0.050 nm) monochromator and a high resolution PGS-2 spectrometer ($f = 200$ cm, resolution 0.015 nm) with photomultiplier tubes: Hamamatsu R-928 and Hamamatsu DH-3, respectively. A quartz achromatic lens was applied to focus the plasma radiation into the entrance slits of the monochromator/spectrometer. The sensitivity of the optical systems versus the wavelength was calibrated with the aid of the Bentham halogen lamp (the Protection Engineering Ltd. certificate in the 250–800 nm spectral range).

3. Results and discussion

3.1. Identification of plasma components

The spectra of N_2–H_2 and N_2–H_2–TIP were measured in the range of 200–800 nm wavelength. The identification of atoms and diatomic molecules was carried out with the aid of the NIST Atomic Spectra Database [20] and the Pearce and Gaydon molecular spectra table [21]. Numerous bands of N_2 (strong $C^3\Pi_u$–$B^3\Pi_g$ system and weak $B^3\Pi_g$–$A^3\Sigma_u^+$ system) and strong bands of N_2^+ ($B^2\Sigma^+$–$X^2\Sigma^+$ system) were detected in the N_2–H_2 plasma. The most intense spectra were the (0–0) bandhead of the N_2^+ ($B^2\Sigma^+$–$X^2\Sigma^+$) system and the (0–2) and (0–0) bands of N_2 of the $C^3\Pi_u$–$B^3\Pi_g$ system. Strong hydrogen lines (H_α at 656.28 nm and H_β at 486.13 nm) were observed. The next hydrogen line, i.e. H_γ at 434.14 nm was not clearly identified due to the overlapping by the $C^3\Pi_u$–$B^3\Pi_g$ (0–4) band of N_2 at 434.36 nm. Some weak nitrogen lines: the atomic N I at 742.4, 744.2, 746.8 and 818.8 nm and the ionic N II at 500.1, 500.5, 567.6 and 567.9 nm were detected. Additionally, the $A^3\Pi_g$–$X^3\Sigma^-$ (0–0) NH bandhead at 336.0 nm, partially overlapped by the strong (0–0) $C^3\Pi_u$–$B^3\Pi_g$ band of N_2 with the bandhead at 337.13 nm was also noticed.

The introduction of evaporated TIP into nitrogen–hydrogen plasma zone resulted in the emission of CN spectra (the most intense bands of the violet system $B^2\Sigma^+$–$X^2\Sigma^+$ and very weak of the red system $A^2\Sigma$–$X^2\Sigma$), CO (the $B^1\Sigma$–$A^1\Pi$ bands at 519.82 nm (0–2), 483.53 nm (0–1) and 451.09 (0–0)), CH ($A^2\Delta$–$X^2\Pi$ (0–0) band at 431.4 nm) (see Fig. 1) and C I line (at 247.86 nm) species. Additionally, the weak spectra of C_2 belonging to the $A^3\Pi_g$–$X'^3\Pi_u$ transition with the band heads at 473.71 nm (1–0), 471.52 nm (2–1), 512.93 nm (1–1) and 516.52 (0–0) and the weak spectra of CO^+ ($B^2\Sigma^+$–$X^2\Sigma^+$) in the 210–250 nm spectra region (the band heads at 211.24 nm (1–0), 218.98 nm (0–0), 229.96 nm (0–1), 232.52 nm (1–2)) were also identified.

In contrast to the emission of spectra of the rf and dc plasmas with $TiCl_4$ [4,5,7,8], we did not observe any atomic and ionic lines of titanium. It indicates that the

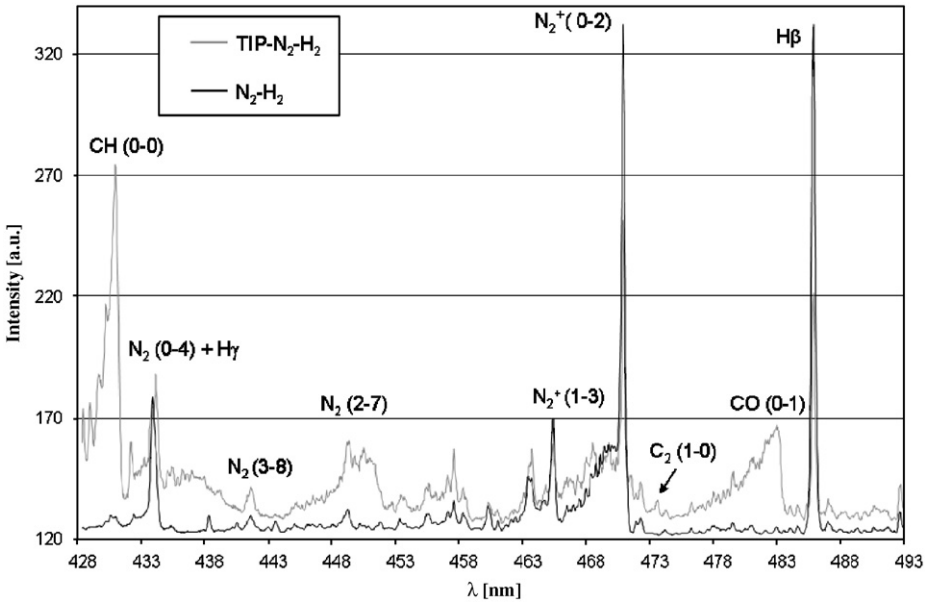

Fig. 1. Optical emission spectra from the N_2–H_2 (black solid) and the N_2–H_2–TIP (gray solid) mixtures.

Table 1
Spectroscopic data of the examined species

Species	Transition	Wavelength (nm)	Threshold energy (eV)
Ar	$2p^1$–$1s^2$	750.39	13.48
C	$3s^1$ (^{3}P) 4p–$3p^4$ (^{3}P) 4s	247.86	7.68
H	$4d^2D^0_{3/2} - 2p^2P^0_{1/2}$	468.13	12.8
N	$2p^2(^3P)3p$–$2p^2(^3P)3s$	821.88	11.84
CO	(0–1) $B^1\Sigma$–$A^1\Pi$	483.53	10.8
CH	(0–0) $A^2\Delta$–$X^2\Pi$	431.40	2.88; ~12[a]
CN	(0–0) $B^2\Sigma^+$–$X^2\Sigma^+$	388.43	3.2
N_2	(0–2) $C^3\Pi_u$–$B^3\Pi_g$	380.20	11.2
N_2^+	(0–0) $B^2\Sigma^+_u$–$X^2\Sigma^+_g$	391.44	18.7

[a]Threshold energy for the production of CH(A).

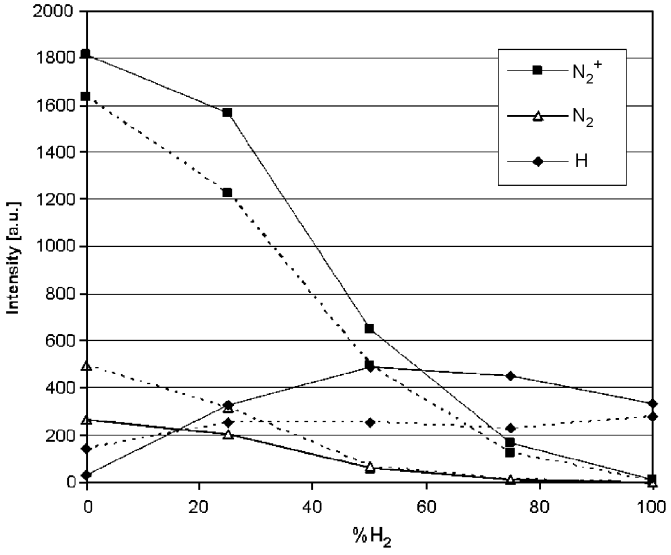

Fig. 2. The emission intensity of N_2^+, N_2 and H in the N_2–H_2 (solid line) and the N_2–H_2–TIP (broken line) mixtures.

decomposition degree of the titanium MO was less effective than the $TiCl_4$ decomposition and/or the sputtering processes of the deposited thin layers is not effective in the alternating current (100 kHz) glow discharge. As previously, in the dc discharge [18] the spectra of O lines and bands of OH and TiN were not observed here in the 100 kHz discharge.

3.2. Optical emission spectroscopy and actinometry

The following species: N_2^+, N_2, N, CN, CH, C, CO, H may play an important role in the growth processes of layers and in the decomposition processes of titanium isopropoxide. The spectroscopic data of the analyzed species were collected in Table 1. The emission intensities of the analyzed atomic lines and molecular bands were investigated versus the hydrogen concentration in the gas feed (Figs. 2 and 3).

The addition of a titanium MO to the N_2–H_2 plasma caused a fall in the emission intensity of N_2^+ and H (for the mixture containing hydrogen), whereas the emission intensity of N_2 was clearly higher for the mixtures containing 0% and 25% H_2 (Fig. 2). The increase in hydrogen concentrations in the TIP–N_2–H_2 mixture resulted in the fall in the emission intensities of N_2^+, N_2 and N (Fig. 2) and CH, CN (Fig. 3). The change of hydrogen concentration from 25% to 100% led to an increase in the emission intensities of C I line, while the emission intensities of H and CO were practically independent from the hydrogen concentration in the analyzed mixture.

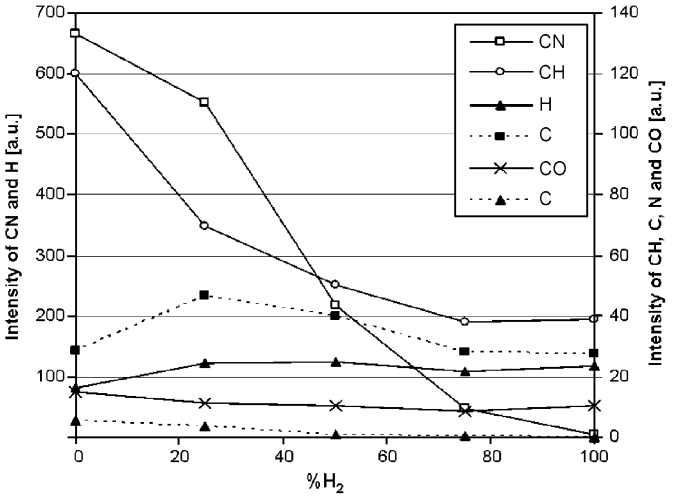

Fig. 3. The emission intensities of selected species versus the hydrogen concentration in the N_2–H_2–TIP mixture.

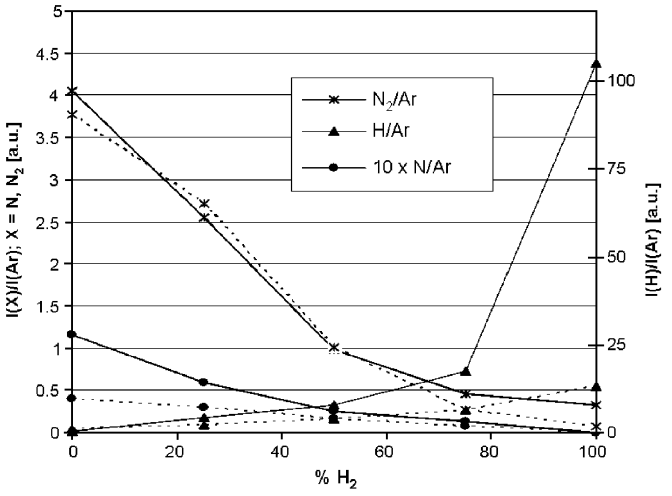

Fig. 4. The relative concentrations of H, N_2 and N species in the N_2–H_2 (solid line) and the N_2–H_2–TIP (broken line) mixtures.

The optical actinometry technique [16,22,23] was applied here to study the H, C, N, CH, CO, N_2 and CN relative concentration in the analyzed mixtures. This technique is based on monitoring the emission intensity variation of lines of inert gases so-called actinometer (Act) and of some lines or bandheads of the species of interest [16]. The concentration of the plasma component (X) is evaluated from the ratio of emission intensity: $I(X)/I(Act)$, where $I(Act)$ is the actinometer emission intensity. The actinometry technique was validated by an independent measurement of species concentration only for H, N, N_2 [24,25]. Nevertheless, for the other species (X = CH, CN, CO, C), the ratio of the emission intensity: $I(X)/I(Act)$, has been considered as a good representation of the evolution of their relative concentration [22,23,26]. Argon was chosen as actinometer and the Ar I line at 730.39 nm was selected here, considering that its threshold energy was close to the threshold energy of H, CO, N_2, N and the CH species (see Table 1). As in the earlier works [17,23] we also applied the optical actinometry technique so as to evaluate the CN and C relative concentration in the reactive mixture. The quantity of the introduced actinometer (i.e. argon) was 4%.

The concentration of H, N_2 and N species were compared for the N_2–H_2 and N_2–H_2–TIP plasma as a function of hydrogen concentration. The N_2 and N relative concentration decrease and the H relative concentration increase in the growth of the hydrogen contribution in the analyzed mixtures were observed as shown in Fig. 4. The introduction of TIP to the N_2–H_2 mixture did not cause any significant changes of the N_2 relative concentration (for the mixture containing nitrogen) and caused the fall in H and N concentrations. It may suggest that H radicals play an important role in the reaction involving titanium isopropoxide or/and the by-product coming from the titanium compound. Fig. 5 shows the H, N_2, CN, CH, CO, C, N relative concentrations for the N_2–H_2–TIP

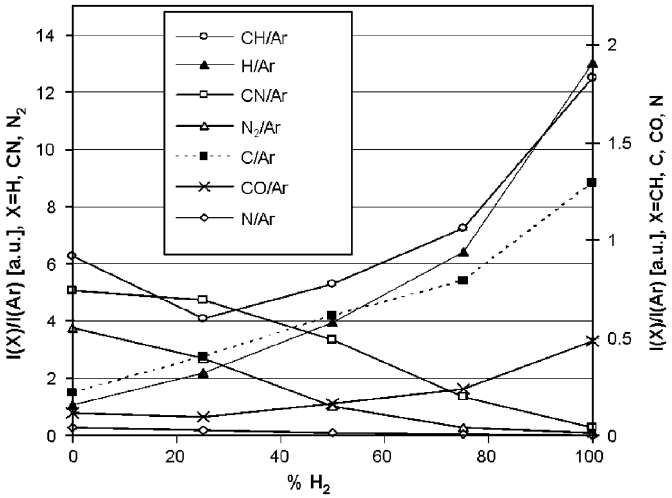

Fig. 5. The relative concentrations of H, CO, N_2, CN, CH, C and N in the titanium isopropoxide–nitrogen–hydrogen mixture.

mixture versus the percentage of hydrogen. The increase in the hydrogen fraction from 0% to 75% in the nitrogen–hydrogen mixture, caused a growth of the concentration of H atoms as well as other species coming from the $Ti[OCH(CH_3)_2]_4$ decomposition processes, i.e. CO, CH and C. Our results indicate that a major source of H atoms is provided by the dissociation process of molecular hydrogen, which is a component of the analyzed mixture. On the other hand, the growth concentration of CO, CH and C species with the hydrogen fraction in the mixture may indicate that hydrogen is responsible for cracking some bonds in titanium isopropoxide (and/or by-products coming from titanium isopropoxide, e.g. acetone (CH_3COCH_3) [9]). The N_2 and CN relative concentrations decreased in a similar manner with the growth of the hydrogen fraction in the N_2–H_2–TIP mixture.

Table 2
The electron excitation, vibrational and rotational temperatures in the N_2–H_2 and N_2–H_2–TIP mixtures versus the percentage of H_2

% H_2	N_2–H_2 mixture					N_2–H_2–Ti[OCH$(CH_3)_2]_4$ mixture				
	100%	75%	50%	25%	0%	100%	75%	50%	25%	0%
T_{exc}(H) (K)	6600	6640	6730	7260	9690	5740	6290	6400	6470	7430
T_{vib}(CN) (K)	–	–	–	–	–	8120±900	6110±230	5440±360	4710±140	4740±310
$T_{vib}(N_2)$ (K)	–	3250±250	3060±210	2880±220	2970±200	–	3060±230	2910±290	2850±270	2730±230
$T_{vib}(N_2^+)$ (K)	–	1480	1510	1660	1770	–	1480	1500	1590	1620
$T_{rot}(N_2^+)$ (K)	–	535±10	660±30	700±20	790±10	–	660±30	670±20	890±30	840±20

3.3. Plasma diagnostics

Under the assumption of a local thermal equilibrium (LTE) or the partial LTE (p-LTE) state, the excitation temperature (T_{exc}) is considered to be in concord with the electron temperature (T_e), namely $T_{exc} \approx T_e$. The rotational temperature (T_{rot}) is the key parameter in the plasma processes, because it is assumed to be close to the gas (kinetic) temperature [16]. The plasma diagnostics were conducted for the discharges in the N_2–H_2 and N_2–H_2–Ti[OCH$(CH_3)_2]_4$ reactive mixture. The excitation, the vibrational and rotational temperatures as well as the electron number density were measured as a function of hydrogen concentration in the analyzed mixtures.

The electron excitation temperature (T_{exc}) was determined using the well-known two-line intensity ratio method [1]:

$$\frac{I_1}{I_2} = \left(\frac{g_1 A_1 \lambda_2}{g_2 A_2 \lambda_1}\right) - \exp\left(\frac{E_1 - E_2}{kT_{exc}}\right), \quad (1)$$

where I is the emission intensity of line, g the statistical weight, A the transition probability, λ the wavelength of light emitted species, E the energy of the upper levels, and k the Boltzmann constant. The two lines of hydrogen, H_α and H_β, with the energies 12.1 and 12.8 eV, respectively, were used.

The vibrational temperatures (T_{vib}) of CN, N_2 and N_2^+ were calculated with the aid of the Boltzmann plot method, from the following equation [1,19]:

$$\ln\left(\frac{I_{v'v''}}{q_{v'v''}\nu^4_{v'v''}}\right) = C - \frac{G(v')}{kT_{vib}}, \quad (2)$$

where $I_{v'v''}$ is the intensity of the vibrational bands, $q_{v'v''}$ the Franck–Condon factor, ν the transition frequency, $G(v')$ the vibrational energy of the upper state, v the vibrational quantum number, and C a constant.

The plot $\ln(I_{v'v''}/(q_{v'v''}\nu^4))$ as a function of $G(v')$ (the Boltzmann plot method) provides a straight line with a slope equal to $-1/kT_{vib}$.

The six bands of $C^3\Pi_u$–$B^3\Pi_g$ system of N_2, i.e. (0–2), (1–3), (2–4), (1–0), (2–1) and (3–2), four bands of $B^2\Sigma^+$–$X^2\Sigma^+$ system of CN, i.e. (0–0), (1–1), (2–2) and (3–3), and two bands of $B^2\Sigma^+$–$X^2\Sigma^+$ of N_2^+, i.e. (0–1) and (1–2), were employed. All the band head intensities were measured considering the background corrections, separately for each band.

The T_{rot} was calculated from the R-branch of the (0–0) band of the N_2^+ molecules, using the Boltzmann plot method [1,19]:

$$\ln\left(\frac{I_{K'K''}}{K' + K'' + 1}\right) = C - \frac{F(K')}{kT_{rot}}, \quad (3)$$

where $I_{K'K''}$ is the rotational line intensity, $F(K')$ the energy of the upper rotational state, K', K'' the rotational quantum numbers of the upper and lower states, and C a constant.

The rotational structure of the (0–0) band of N_2^+ was recorded in the fifth order by means of high resolution spectrometer. The rotational lines of the R-branch with rotational quantum numbers (K') from 4 to 21 were applied.

The spectroscopic method, based mainly on the Stark broadening of hydrogen lines, was applied for investigation of the electron number density in various types of the low-pressure plasmas [27,28]. The electron number densities (n_e) were calculated here from the Stark broadening of the H_β line at 486.133 nm. The full-width at half-maximum (FWHM) of the H_β line due to the Stark effect ($\Delta\lambda_{1/2}$) is related to the electron number density (n_e), according to the Griem formula, i.e. $n_e = C(\mathrm{Ne,Te}) \times (\Delta\lambda_{1/2})^{3/2}$ [29], where $C(N_e,T_e) = 3.58\,0^{14}\,\text{Å}^{-3/2}\,\mathrm{cm}^{-3}$ is a constant. The H_β line was measured by means of the high-resolution spectrometer in the second order (resolution: 128 pixels nm^{-1}). The experimental profile of H_β was fitted by the Lorentz algorithm by means of the Origin computer program (version 6.0). In order to measure exactly the Stark broadening, the H_β FWHM was corrected for the instrumental and the Doppler broadening (~0.032 nm).

The relative standard of deviation uncertainties for T_{exc}, T_{vib} and T_{rot} were evaluated to be at the level of ~10%, 3–10% and 1–5%, respectively. The other details on the calculation of the excitation, vibrational and rotational temperatures and the electron number density were described and presented in the earlier works [16,19].

Table 2 illustrates the excitation, vibrational and rotational temperatures for N_2–H_2 and N_2–H_2–TIP mixtures versus the hydrogen concentration. Generally, the introduction of TIP into the N_2–H_2 plasma resulted in lowering the H excitation temperature and the vibrational temperatures of N_2 and the increase in the rotational

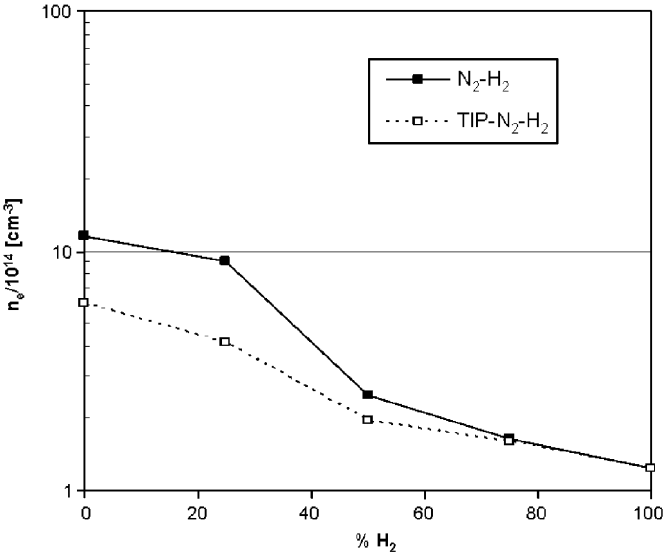

Fig. 6. The electron number density for the N_2–H_2 (solid line) and the N_2–H_2–TIP (broken line) mixtures.

temperature of N_2^+. The observed increase in the rotational (gas) temperature is not very significant and it may be due to the introduction of the hot vapor of titanium isopropoxide (heated up to 60 °C) into the plasma zone. In the mixture containing TIP and nitrogen, the H excitation temperature was higher than vibrational temperature of CN. On the other hand, the values of the vibrational temperature of CN were considerably higher than those for N_2 and N_2^+. It is perhaps caused by the non-equilibrium state of the analyzed plasma. In conclusion, the following relation between the temperatures in the mixtures containing nitrogen was observed:

$$T_{exc}(H) \geqslant T_{vib}(CN) > T_{vib}(N_2) > T_{vib}(N_2^+) > T_{rot}(N_2^+).$$

The excitation temperature of H and the vibrational temperature of the CN were sensitive to changes in the plasma gas composition, whereas the vibrational temperatures of N_2 and N_2^+ slightly increased with the growth of the fraction of hydrogen in the TIP–N_2–H_2 mixture (Table 2).

The electron number density versus the hydrogen concentration is presented in Fig. 6. For both of the analyzed mixtures, i.e. N_2–H_2 and N_2–H_2–TIP, the electron number density decreased with the growth of the hydrogen concentration in the mixture. The addition of TIP to the nitrogen–hydrogen mixture caused the lowering of the electron number density. This effect was not observed for the plasma rich in hydrogen (75% and 100%), where probably hydrogen plays an essential role in the decomposition processes of titanium isopropoxide.

4. Summary

The decomposition of titanium isopropoxide in nitrogen–hydrogen 100 kHz plasma was investigated by means of OES and the optical actinometry technique. The relative concentrations of H, CO, CH and C species increased with the growth of the hydrogen fraction in nitrogen–hydrogen mixture. The results indicate that hydrogen is responsible for cracking of some bonds in the $Ti[OCH(CH_3)_2]_4$ molecule, especially in rich hydrogen plasmas. The measurements of the excitation, vibrational and rotational temperatures showed significant differences between them. It exemplifies well that the low pressure mid-frequency (100 kHz) plasma is far from the equilibrium state. The electron densities as well as the temperatures were found to be related to the chemical composition of the reactive mixture.

References

[1] Konuma M. Films deposition by plasma techniques. Berlin: Springer; 1992.
[2] Weber A, Poeckelmann R, Klages CP. Appl Phys Lett 1995;67:2934.
[3] Boo JH, Heo CH, Cho YK, Han JG. J Vac Sci Technol A 2000; 18:1590.
[4] Mogensen KS, Eskildsen SS, Mathiansen C, Bøttiger J. Surf Coat Technol 1998;102:41.
[5] Peter S, Richter F, Tabersky R, Konig U. Thin Solid Films 2001; 398–399:343.
[6] Rodrigo AB, Lasorsa C, Shimozuma M, Alvarez F, Perillo P. J Phys D: Appl Phys 1997;30:2397.
[7] Peter S, Richter F, Tabersky R, Konig U. Thin Solid Films 2000; 377–378:430.
[8] Ishii Y, Shibata T, Yoshino Y, Ichimura H, Kobayashi K. J Ceram Soc Jpn 1992;100:1184.
[9] Weber A, Poeckelmann R, Klages CP. Microelectron Eng 1997; 33:277.
[10] Wierzchon T, Sobiecki JR. Surf Coat Technol 1998;98:1455.
[11] Sobiecki JR, Mankowski P, Wierzchon T. Vacuum 2003;68:105.
[12] Yun JY, Rhee SW, Park S, Lee JG. J Vac Sci Technol A 2000; 18:2822.
[13] Peters AM, Nastasi M. Vacuum 2002;67:169.
[14] Kim SK, Kim TH, Wohle J, Rie RT. Surf Coat Technol 2000; 131:121.
[15] Xiao ZG, Mantei TD. Surf Coat Technol 2004;177–178:389.
[16] Jamroz P, Zyrnicki W. Eur Phys J Appl Phys 2002;19:201.
[17] Jamroz P, Zyrnicki W. Diamond Relat Mater 2005;14:1498.
[18] Kulakowska-Pawlak B, Zyrnicki W. Thin Solid Films 1995;266:8.
[19] Jamroz P, Zyrnicki W. Surf Coat Technol 2006;201:1444.
[20] NIST Atomic Spectra Database: 〈http://physics.nist.gov/PhysRefData/ASD/index.html〉.
[21] Pearce RWB, Gaydon AG. The identification of molecular spectra. London: Chapman & Hall; 1976.
[22] Durrant SF, De Moraes MAB, Mota RP. Vacuum 1996;47:187.
[23] Fabia F, Creatore M, Palumbo F, Colaprico V, d'Agostino R. Surf Coat Technol 2001;142–144:1.
[24] Gicquel A, Chenevier M, Hassouni Kh, Tserepi A, Dubus M. J Appl Phys 1998;83:7504.
[25] Henriques J, Villeger S, Levaton J, Nagai J, Santana S, Amorim J, et al. Surf Coat Technol 2005;200:814.
[26] Durrant SF, De Moraes MAB. J Vac Sci Technol A 1995;13:2513.
[27] Acon BW, Chantal Stehle Ch, Zhang H, Montaser A. Spectrochim Acta Part B 2001;56:527.
[28] Ivkovic M, Jovicevic S, Konjevic N. Spectrochim Acta Part B 2004; 59:591.
[29] Griem HR. Plasma spectroscopy. New York: McGraw-Hill; 1964.